Bioorganic Chemistry 93 (2019) 102747

Contents lists available at ScienceDirect

Bioorganic Chemistry

journal homepage: www.elsevier.com/locate/bioorg

Bioconversion of xylose to xylonic acid via co-immobilized dehydrogenases for conjunct cofactor regeneration☆

Karolina Bachosz[a], Karol Synoradzki[b,c], Maciej Staszak[a], Manuel Pinelo[d], Anne S. Meyer[e], Jakub Zdarta[a,*,1], Teofil Jesionowski[a,*,2]

[a] Institute of Chemical Technology and Engineering, Faculty of Chemical Technology, Poznan University of Technology, Berdychowo 4, PL-60965 Poznan, Poland
[b] Institute of Molecular Physics, Polish Academy of Sciences, Smoluchowskiego 17, PL-60179 Poznan, Poland
[c] Institute of Low Temperature and Structure Research, Polish Academy of Sciences, Okolna 2, PL-50422 Wroclaw, Poland
[d] Department of Chemical and Biochemical Engineering, DTU Chemical Engineering, Technical University of Denmark, Soltofts Plads 229, DK-2800 Kgs. Lyngby, Denmark
[e] Department of Biotechnology and Biomedicine, DTU Bioengineering, Technical University of Denmark, Soltofts Plads 227, DK-2800 Kgs. Lyngby, Denmark

ARTICLE INFO

Keywords:
Xylose dehydrogenase
Alcohol dehydrogenase
Enzyme co-immobilization
Enzyme stability
Xylose conversion
NADH
Cofactor regeneration system

ABSTRACT

Enzymatic cofactor-dependent conversion of monosaccharides can be used in the bioproduction of value-added compounds. In this study, we demonstrate co-immobilization of xylose dehydrogenase (XDH, EC 1.1.1.175) and alcohol dehydrogenase (ADH, EC 1.1.1.1) using magnetite-silica core-shell particles for simultaneous conversion of xylose into xylonic acid (XA) and *in situ* cofactor regeneration. The reaction conditions were optimized by factorial design, and were found to be: XDH:ADH ratio 2:1, temperature 25 °C, pH 7, and process duration 60 min. Under these conditions enzymatic production of xylonic acid exceeded 4.1 mM and was more than 25% higher than in the case of a free enzymes system. Moreover, the pH and temperature tolerance as well as the thermo- and storage stability of the co-immobilized enzymes were significantly enhanced. Co-immobilized XDH and ADH make it possible to obtain higher xylonic acid concentration over broad ranges of pH (6–8) and temperature (15–35 °C) as compared to free enzymes, and retained over 60% of their initial activity after 20 days of storage. In addition, the half-life of the co-immobilized system was 4.5 times longer, and the inactivation constant (k_D = 0.0141 1/min) four times smaller, than those of the free biocatalysts (k_D = 0.0046 1/min). Furthermore, after five reaction cycles, immobilized XDH and ADH retained over 65% of their initial properties, with a final biocatalytic productivity of 1.65 mM of xylonic acid per 1 U of co-immobilized XDH. The results demonstrate the advantages of the use of co-immobilized enzymes over a free enzyme system in terms of enhanced activity and stability.

1. Introduction

Biocatalysis is attracting increasing attention in modern chemical synthesis, and the use of microbes and/or enzymes isolated from them is of particular interest for both environmental and economic reasons [1,2]. Enzymatic reactions are frequently used in the production processes of pharmaceuticals, herbicides or energy raw materials from biomass [3]. The progress and rapid development of biocatalyst-based reactions are stimulated by several advantages compared with traditional chemical catalysis, including mild process conditions, high chemo-, regio- and enantioselectivity, absence of side reactions and by-products, and the limited quantity of undesired isomers. Moreover, enzymatic processes are usually carried out in water or buffer solutions; thus, the use of toxic, volatile solvents is unnecessary [3–5].

Despite the benefits of biocatalytic processes, there are also a number of disadvantages that diminish the practical application of enzymes on an industrial scale, such as the low commercial availability and high price of enzymes, as well as their poor stability and relatively rapid loss of biocatalytic activity [2]. These problems can be effectively overcome with the use of enzyme immobilization, which makes it possible to improve the stability and reusability of biocatalysts, as well as increasing their biocatalytic productivity [6,7]. However, the key step in obtaining efficient biocatalytic systems is the selection of the support material. In choosing the most suitable matrix, consideration

☆ Papers selected for publication under the virtual special issue Enzymatic systems towards synthesis of biologically active compounds.

* Corresponding authors.
E-mail addresses: jakub.zdarta@put.poznan.pl (J. Zdarta), teofil.jesionowski@put.poznan.pl (T. Jesionowski).
[1] ORCID-id: 0000-0003-0268-2116.
[2] ORCID-id: 0000-0002-7808-8060.

https://doi.org/10.1016/j.bioorg.2019.01.043
Received 8 November 2018; Received in revised form 14 January 2019; Accepted 18 January 2019
Available online 07 February 2019
0045-2068/

should be given to such factors as the biochemical properties of the enzyme, the type of catalyzed reaction, physicochemical features of the support, and its stability [8–10]. Over recent years there has been growing interest in the application of composite materials as supports for enzyme immobilization, due to their tailored and designable properties. A prime example of such a material are magnetite-silica core-shell particles. This material is characterized by a large specific surface area and the presence of many hydroxyl groups on the surface, which facilitate binding of the enzyme. Moreover, the magnetic core of the particles enhances separation of the immobilized enzymes from the reaction mixture; this improves the purity of the products and reduces process costs [11]. This material is therefore attracting attention for use not only as a support for enzyme immobilization, but also as a drug delivery system, as well as in various branches of biotechnology and biomedicine, mainly due to the simplicity and relatively low costs of its synthesis.

Oxidoreductases, and notably dehydrogenases, have not been widely used in saccharide upgrading or in large-scale industrial conversion, mainly because of the cofactor requirement. For the proper action of dehydrogenase, the presence of non-protein cofactors in the reaction system is required, as cofactors are responsible for electron transfer [2]. Recently reported data on cofactor recycling and microbial dehydrogenase robustness now appear promising. The presence of these substances in the reaction mixture, participating in oxidation and/or reduction reactions, is necessary not only for the biocatalyst to maintain its catalytic properties, but also to prevent undesired modifications in the enzyme structure [12]. However, due to the high price and the fact that the enzymatic cofactors are exhausted during the process, the concept has been developed of biocatalytic systems that will enable the regeneration of cofactors and simultaneously increase the efficiency and productivity of the biotransformations [13]. Effective cofactor regeneration may be achieved, for example, by the synergistic coupling of two (or more) biocatalysts which catalyze two parallel reactions [14]. In one of them the cofactor is used up, and in the other the cofactor is regenerated. For instance, Zheng et al. (2011) [13] created a system based on glucose dehydrogenase and glutamate dehydrogenase, which effectively regenerates NADH, and converts glucose into glutamate and D-glucono-1,5-lactone. Rehn et al. (2016) [15] used alcohol dehydrogenase and NADH oxidase to oxidize alcohols with the simultaneous regeneration of NAD(P)+. In another study, Wang et al. (2013) [16] carried out the regeneration of NADH, required for transformation of diacetyl into 2,3-butanediol, using a biocatalytic system based on three enzymes: 3-butanediol dehydrogenase, formate dehydrogenase and glucose dehydrogenase. Three reactions took place in parallel, and additionally, from the NADH regeneration, carbon dioxide and gluconic acid were obtained as by-products.

Enzymatic cofactors also play an important role in the biocatalytic conversion of selected biomass components, as alternative raw materials for the production of a wide range of chemicals. Among others, of particular interest is xylose, one of the main product of biomass pretreatment. Xylose can be converted in enzyme-catalyzed reactions to obtain valuable chemical compounds with high application potential [17,18]. For instance, xylose could be transformed into xylitol, a compound frequently used in the food and pharmaceutical industries, using the NADPH-dependent xylose reductase. Also other compounds, such as xylonic acid (XA) and xylulose, could be formed by the conversion of xylose using various NADH-dependent dehydrogenases [19,20]. Xylonic acid is mentioned among the 30 most valuable chemicals obtaining from biomass [21]. This is proven by the numerous of possible application mainly in food, agriculture and pharmaceutical industries [22]. Among others, XA is used as a precursor in the synthesis of D-1,2,4-butanetriol, as a biopesticide or as a cement dispersing agent to reduce amount of water in concrete [23,24]. Furthermore, it has been proven, that xylonic acid enhances absorption of vitamin C [25]. However, due to practical difficulties, commercial production of xylonic acid is limited. The most commonly used method for synthesis of the above-mentioned acid is convertion of D-xylose into xylono-γ-lactone in the presence of xylose dehydrogenase, followed by spontaneous hydrolysis of xylono-γ-lactone to xylonic acid. This process can be carried out with high yields using bacterial species, such as *Pseudomonas* and *Gluconobacter*, in particular *Pseudomonas frags* and *Gluconobacter oxydans* [26]. However, the use of enzymes of bacterial origin results in the necessity of thorough pre-treatment of the lignocellulosic material and the proper selection of pH, due to the sensitivity of the biocatalysts to the acidic conditions [27]. To minimize disadvantages of the use of bacterial enzymes, conversion of xylose could be carried out using biocatalysts of fungal origin, i.e. *Trichoderma viridea* or *Pichia querquum*, because of their low nutritional requirements and relatively high resistance to inhibitors [28]. In addition, the process efficiency can also be improved by the use of bipolar membrane electrodialysis [29]. Nevertheless, it should be emphasized that based on a results of economic and technical analyses, depending on the used method, the minimum product selling price may be in the range of 0.17–0.41 USD per kg of xylonic acid [30,31].

Nevertheless, the enzyme-based processes of xylose conversion required the addition of a new portion of cofactor for their efficient and continuous running. An interesting solution to this problem was suggested by Marpani et al. (2017) [32], who developed a system in which xylose is converted to xylonic acid with simultaneous conversion of formaldehyde to methanol, using, respectively NAD+-dependent xylose dehydrogenase and NADH-dependent alcohol dehydrogenase. In that study, the reaction kinetics were examined to evaluate the optimal initial concentrations of xylose and formaldehyde. Effective cofactor regeneration was achieved, providing a basis for further studies in this area of biotechnology.

As has been described, studies on effective cofactor regeneration systems have already been undertaken. However, they suffer from insufficient enzyme stability and, in consequence, low cofactor regeneration efficiency. Thus, in the present work, for the first time, we present a proof-of-concept for the co-immobilization of xylose dehydrogenase (EC 1.1.1.175) and alcohol dehydrogenase from *Saccharomyces cerevisiae* (EC 1.1.1.1) using magnetite-silica core-shell particles as a support material, and an application in the conversion of xylose and simultaneous *in situ* cofactor regeneration, as shown in Scheme 1. The synthesized support material is comprehensively analyzed, and the optimal ratio of co-immobilized XDH to ADH is determined. Finally, a practical application of the XDH/ADH system is evaluated, based on the continuous conversion of xylose and simultaneous cofactor regeneration. Moreover, the effect of pH and temperature on the efficiency of xylonic acid production and the stability of the above-mentioned system, as well as its reusability and biocatalytic productivity over consecutive catalytic cycles, have been studied in details. The data presented might provide guidance for the development and application of cofactor regeneration systems for use in the conversion of biomass components. However, these studies may be further developed to enhance conversion of xylose and improve cofactor regeneration. This might be achieved by the use of periodic and continuous bioreactors to ensure constant supply of substrates and removal of products. Furthermore, membrane processes could be applied for efficient separation of the obtained products. Finally, to enhance efficient cofactor regeneration, other enzymes, i.e. NADH oxidase or lactate dehydrogenase could be applied as well as cofactor immobilization might be carried out. Nevertheless, further studies covering all of the aforementioned aspects should be performed to find the optimal solutions.

2. Materials and methods

2.1. Chemicals and reagents

Iron(III) chloride hexahydrate, iron(II) chloride tetrahydrate, 25% tetramethylammonium hydroxide solution, sodium hydroxide and

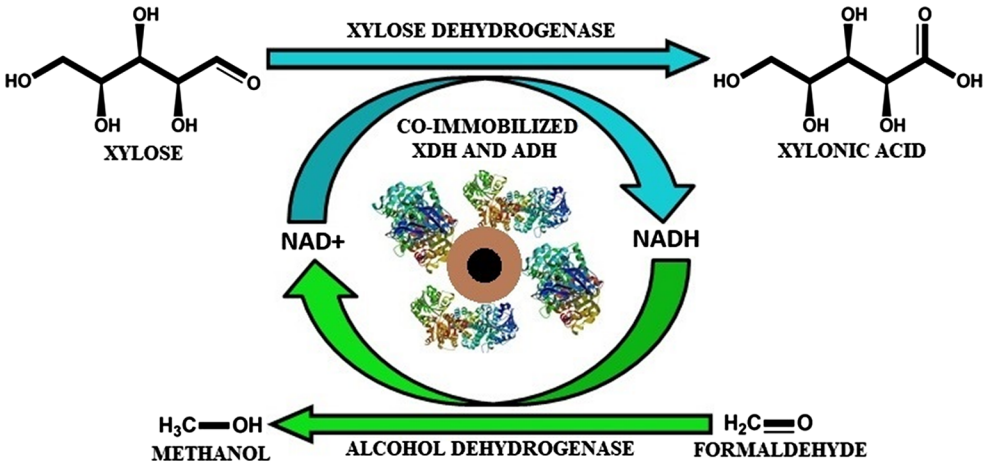

Scheme 1. Simultaneous conversion of xylose into xylonic acid with *in situ* cofactor regeneration catalyzed by co-immobilized xylose dehydrogenase and alcohol dehydrogenase.

tetraethyl orthosilicate (TEOS) used for the synthesis of magnetic nanoparticles and magnetite-silica core shells were obtained from Sigma-Aldrich (USA). Alcohol dehydrogenase from *Saccharomyces cerevisiae* (ADH) (EC 1.1.1.1) was supplied by Sigma-Aldrich (USA), and xylose dehydrogenase (XDH) (EC 1.1.1.175) was supplied by Megazyme (Ireland). 50 mM MES buffer, *β*-nicotinamide adenine dinucleotide hydrate (NAD+), *β*-nicotinamide adenine dinucleotide, reduced disodium salt hydrated (NADH), formaldehyde, ethanol, D-xylose, D-xylonic acid lithium salt and hydrochloric acid were purchased from Sigma-Aldrich (USA).

2.2. Synthesis of magnetite-silica core-shell particles

The magnetite-silica core-shell particles were obtained in a two-step process. In the first stage, magnetite nanoparticles (MNPs) were synthesized according to our previous work [33], using a co-precipitation method with slight modifications. Briefly, $FeCl_2{\cdot}4H_2O$ and $FeCl_3{\cdot}6H_2O$ in a molar ratio of 2:1 were dissolved in water and mixed, using an MS-H-S10 magnetic stirrer (ChemLand, Poland), for 1 h under nitrogen atmosphere at a temperature of 80 °C. During mixing, 20 mL of the tetramethylammonium hydroxide solution was dropped in. After the reaction, magnetic nanoparticles were separated from the mixture using an external magnetic field, washed several times with deionized water and dried at 40 °C for 12 h. In the second step, the previously obtained magnetite nanoparticles were coated in a silica layer. For this purpose, 100 mg of MNPs were dispersed in 100 mL of absolute ethanol:water mixture (4:1 v/v). Further, 0.3 mL of TEOS was added and 3 mL of 1 M NaOH was dropped in during mixing of the solution. The resulting magnetite-silica particles were separated from the reaction mixture using an external magnetic field, washed several times with ethanol and dried at 40 °C for 12 h.

2.3. Immobilization of enzymes

The co-immobilization of ADH and XDH was performed in 50 mM MES buffer at pH 7 and at a temperature of 25 °C. For this purpose, 50 mg of the previously obtained magnetite-silica material was dispersed in 2 mL of buffer solution containing 15 U (0.25 mL) of xylose dehydrogenase and 15 U (0.05 mg) of alcohol dehydrogenase. The resulting mixture was placed in a KS260 Basic incubator (IKA Werke GmbH, Germany) and the process was conducted for 2 h. To identify the most suitable XDH:ADH ratio for effective xylose conversion and cofactor regeneration, immobilization was performed using various initial XDH:ADH ratios (5:1, 2:1, 1:1, 1:2, 1:5). After immobilization, the systems were washed three times with MES buffer to remove unbound protein. Based on the Bradford method [34], using the calibration curve of BSA solutions at known concentrations, the quantity of immobilized enzyme was evaluated (mg/g), as the difference between the initial dosage and final protein concentration in the supernatant after immobilization, per unit mass of support. Also the quantity of the enzyme eluted from the support was examined using the Bradford method.

2.4. Analysis of experimental data

Statistical analysis of the experimental data was performed using the *polyfit* and *polyfitstat* functions in PTC Mathcad mathematical software. For both acid concentration and relative activities, multivariate polynomial regression was applied to model the experimental data. The respective equations used to model acid concentration and activity were:

$$C_{XA}(pH, T) = c_1 + c_2{\cdot}pH + \ c_3{\cdot}T + c_4{\cdot}pH{\cdot}T + c_5{\cdot}pH^2 + c_6{\cdot}T^2 \quad (1)$$

and

$$A(pH, T) = a_1 + a_2{\cdot}pH + a_3{\cdot}T + a_4{\cdot}pH{\cdot}T + a_5{\cdot}pH^2 + a_6{\cdot}T^2 \quad (2)$$

where a_i denotes activity, c_i denotes concentration of xylonic acid, and T denotes temperature. Modelling was performed using the least squares method to find the minimum value of the sum of squared residuals S:

$$S = \sum_{i=1}^{n} (x_{experimental} - x_{model})_i^2 \quad (3)$$

and consequently fitting the functions of the proposed model to the experimental data. An iterative procedure determining the coefficients c_i and a_i was used to satisfy the statistical requirement of minimization of the model residuals. Optimization of the solutions obtained, to find the best conditions for xylonic acid formation, was performed using Maple 16 software.

2.5. Enzymatic conversion of xylose to xylonic acid catalyzed by free and immobilized enzymes

Enzymatic conversion of xylose into xylonic acid with simultaneous cofactor regeneration was performed by equivalent activities of free and co-immobilized enzymes, as presented in Scheme 1. For this purpose, to a reaction mixture containing 5 mM of D-xylose, 5 mM of formaldehyde, 1 mM of NAD+ and 1 mM of NADH in MES buffer at pH 7, 20 U of XDH and 10 U of ADH (XDH to ADH ratio 2:1) of the free or co-immobilized enzymes was added. One enzyme activity unit (U) of free and co-immobilized enzymes was defined as the amount of XDH and

ADH that produced 1 μmol of xylonic acid and methanol, respectively, per minute. The reaction mixture was then shaken on a KS260 Basic incubator (IKA Werke GmbH, Germany) for 60 min at 25 °C. After 60 min of the process, the reaction was terminated by the addition of 1 M HCl. Obtained samples were analyzed by high-performance liquid chromatography (HPLC) to determine concentrations of xylose and xylonic acid.

2.5.1. Effect of pH and temperature on enzymatic conversion of xylose into xylonic acid

The effect of pH and temperature on the bioconversion of xylose (pH and temperature profiles of free and co-immobilized enzymes) was examined using the methodology described above, at pH ranging from 5 to 9 (under optimal temperature conditions) and at temperatures in the range 5–45 °C with a step size of 10 °C (at optimal pH). To adjust the pH of the solution, 0.1 M HCl and 0.1 M NaOH were used. After 60 min, the reaction was terminated and samples were analyzed using HPLC.

2.5.2. Time course of the reaction

The effect of reaction time on the production of xylonic acid by free and co-immobilized enzymes was examined based on the aforementioned reaction of xylose into xylonic acid, carried out under optimal process conditions for 180 min. The mixture was sampled every specified period of time, and the production of XA was evaluated using HPLC.

2.6. Characterization of free and co-immobilized enzymes

2.6.1. Thermostability of free and co-immobilized enzymes

The thermal stability of both free and co-immobilized systems was evaluated based on the catalytic conversion of xylose into xylonic acid as described above, after incubation of samples for a specified period of time (up to 120 min) at a temperature of 25 °C in MES buffer at pH 7.0. After incubation, the systems were used to catalyze the reaction, samples were subjected to HPLC analysis, and the results were used to determine relative activity in terms of xylonic acid production by the free and co-immobilized enzymes. The initial activity of the free and co-immobilized biocatalysts was defined as 100% activity. The inactivation constant (k_D) and half-life ($t_{1/2}$) of the free and co-immobilized systems were evaluated based on the linear regression slope for ln(RA) vs. time.

2.6.2. Storage stability of free and co-immobilized enzymes

The storage stability of the free and co-immobilized enzymes was evaluated over 20 days of storage in MES buffer (pH 7) at 4 °C, based on the reaction of catalytic conversion of xylose into xylonic acid. For the reaction, 20 U of XDH and 10 U of ADH (XDH to ADH ratio 2:1) were used. After the process, samples were analyzed using HPLC, and the results were used to calculate the relative activity. For the purposes of the study of storage stability, the initial value of the activity of the free or co-immobilized enzymes was defined as 100% activity.

2.6.3. Reusability and biocatalytic productivity of co-immobilized enzymes

The reusability of co-immobilized XDH and ADH in the production of xylonic acid was examined over five consecutive reaction cycles. Each cycle lasted 60 min and was carried out under optimal process conditions (pH 7, temperature 25 °C) using a reaction mixture consisting of D-xylose (5 mM), formaldehyde (5 mM), NAD+ (1 mM) and NADH (1 mM). After each reaction cycle, the co-immobilized enzymes were separated from the reaction mixture using an external magnet, washed three times with MES buffer and re-suspended in a new reaction solution. The concentration of xylonic acid after the first catalytic cycle was defined as 100%. The biocatalytic productivity of the co-immobilized enzymes was expressed as a concentration of xylonic acid (mM) produced by the activity of the enzyme system.

2.7. Analytical methods

The magnetic properties of the studied materials were determined using an MPMS (Quantum Design, USA) SQUID magnetometer. Hysteresis curves with magnetic field (μ_0H) up to ± 5 T (50 kOe) were obtained at 5 K and 300 K. Zero-field-cooled (ZFC) and field-cooled (FC) curves were recorded at 0.1 T (1 kOe) magnetic field in a temperature range from 2 K to 300 K.

The morphology of the obtained magnetic nanoparticles and the magnetite-silica core-shell particles before and after immobilization was investigated using transmission electron microscopy (TEM) images recorded using a JEOL JEM-1200EX II (JEOL, USA) instrument at an accelerating voltage of 80 kV.

Fourier transform infrared spectroscopy (FTIR) was used to identify the functional groups present in the materials. Samples were analyzed in the form of KBr pellets formed by mixing 1 mg of the sample with 250 mg of anhydrous potassium bromide, over a wavenumber range of 4000–400 cm^{-1} (resolution 0.5 cm^{-1}) using a Bruker Vertex 70 apparatus (Bruker, Germany).

Enzymatic conversion of xylose into xylonic acid and XA concentration were investigated based on the results of high performance liquid chromatography, performed using equipment from ShimadzuCorp., Japan (LC-20AD, DGU-20A3, SIL-20AC, SCL-10A, CTO-10A). The column system consisted of an Aminex HPX-87H Ion Exclusion Column (300 mm × 8.7 mm) (Bio-Rad) and a guard (H^+) pre-column. The temperature during the analysis was 63 °C, the eluent was 4 mM H_2SO_4 and its flow rate was 0.6 mL/min. Both xylose and xylonic acid were detected using a refractive index detector (RID-10A). Prior to analysis, samples were diluted with the eluent to obtain concentrations of xylose and XA in the ranges 0.05–5 g/L and 0.025–3 g/L respectively.

2.8. Statistical analysis

All measurements were made in triplicate. Error bars are presented as means ± standard deviation. Statistically significant differences were determined using Tukey's test by one-way ANOVA performed in SigmaPlot 12 (Systat Software Inc., USA). Statistical significance was established at the level $p < 0.05$.

3. Results and discussion

3.1. Magnetite-silica particles synthesis and characterization

TEM images were used to investigate the synthesis of the core-shell particles and the morphology and size of the magnetite and magnetite-silica before and after XDH and ADH co-immobilization. The average size of the magnetite particles ranged from 10 to 15 nm (Fig. 1a). The particle diameters of the spheres obtained following silica coating were larger, ranging from 20 to 30 nm (Fig. 1b). This indicates that the magnetic cores were effectively coated by a layer of silica, providing a large surface area for enzyme binding [35]. The mean diameters of the particles did not change significantly following enzyme deposition, indicating that the immobilization process had a negligible effect on the size of the magnetite-silica particles [36].

Coating of the magnetite by silica and effective enzyme immobilization were also confirmed by the results of FTIR analysis (Fig. 2a). The FTIR spectrum of the synthesized magnetite-silica composite contains a signal attributed to Fe–O stretching vibrations at 576 cm^{-1}. There is also a band at 3425 cm^{-1} assigned to stretching vibrations of hydroxyl groups, as well as peaks at 1100 and 805 cm^{-1} corresponding to stretching and bending vibrations respectively of Si—O—Si bonds, proving the effective formation of the expected support material [37]. After enzyme co-immobilization, the absorption peak with a maximum at 1645 cm^{-1} increased in intensity, and a signal appeared at 1555 cm^{-1}; these correspond to amide I and amide II

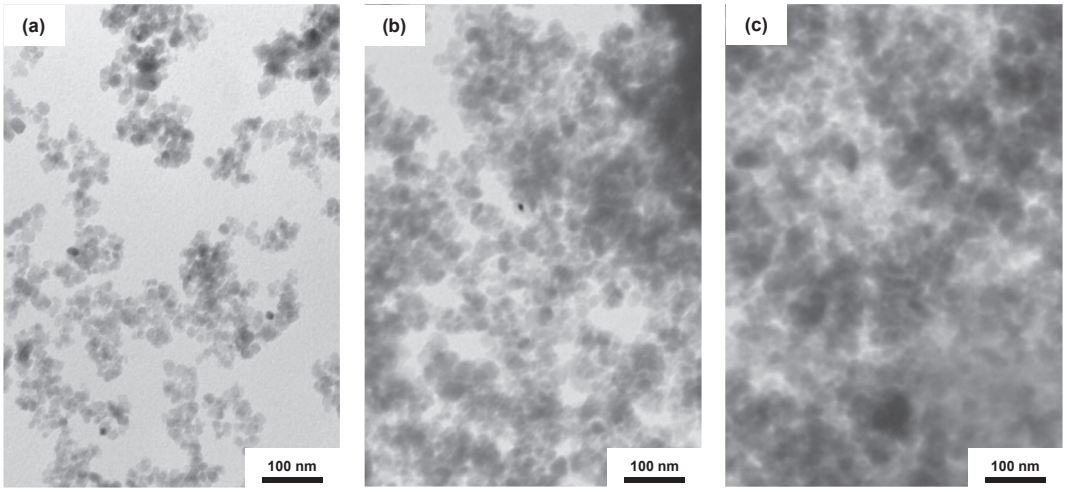

Fig. 1. TEM images of (a) synthesized magnetite nanoparticles, (b) magnetite-silica core-shell particles and (c) the system obtained after enzyme co-immobilization.

stretching vibrations, characteristic for the peptide structure of xylose and alcohol dehydrogenase. Moreover, appearance of signal at 1452 cm^{-1} and increase in the intensity of signal with maximum at 2950 cm^{-1} has also been observed. These peaks are attributed to stretching vibrations of C—H bonds, which form the skeleton of the enzyme structure. Thus, it can be concluded that both enzymes were successfully deposited onto the surface of the magnetite-silica core-shell particles [38].

The magnetic properties of the studied materials are presented in Fig. 2b and indicate superparamagnetic behaviour at room temperature for all samples. The magnetic field dependence of the magnetization, M (μ_0H), measured at 300 K, shows no hysteresis. The shape of $M(\mu_0 H)$ is typical for ferromagnetic materials. In fields stronger than 0.5 T, magnetization saturates at values smaller than the value for bulk Fe_3O_4, due to the combined effect of size and surface. Additionally, the increase in the thickness of the shell layer surrounding the magnetic core in the Fe_3O_4-SiO_2 core-shell particles can lead to reduction of the magnetization values, as suggested in our earlier work [39]. At 5 K, the hysteresis loop of the Fe_3O_4 shows a non-zero coercivity and remanence (lower inset of Fig. 2b), implying that the iron nanoparticles are in a

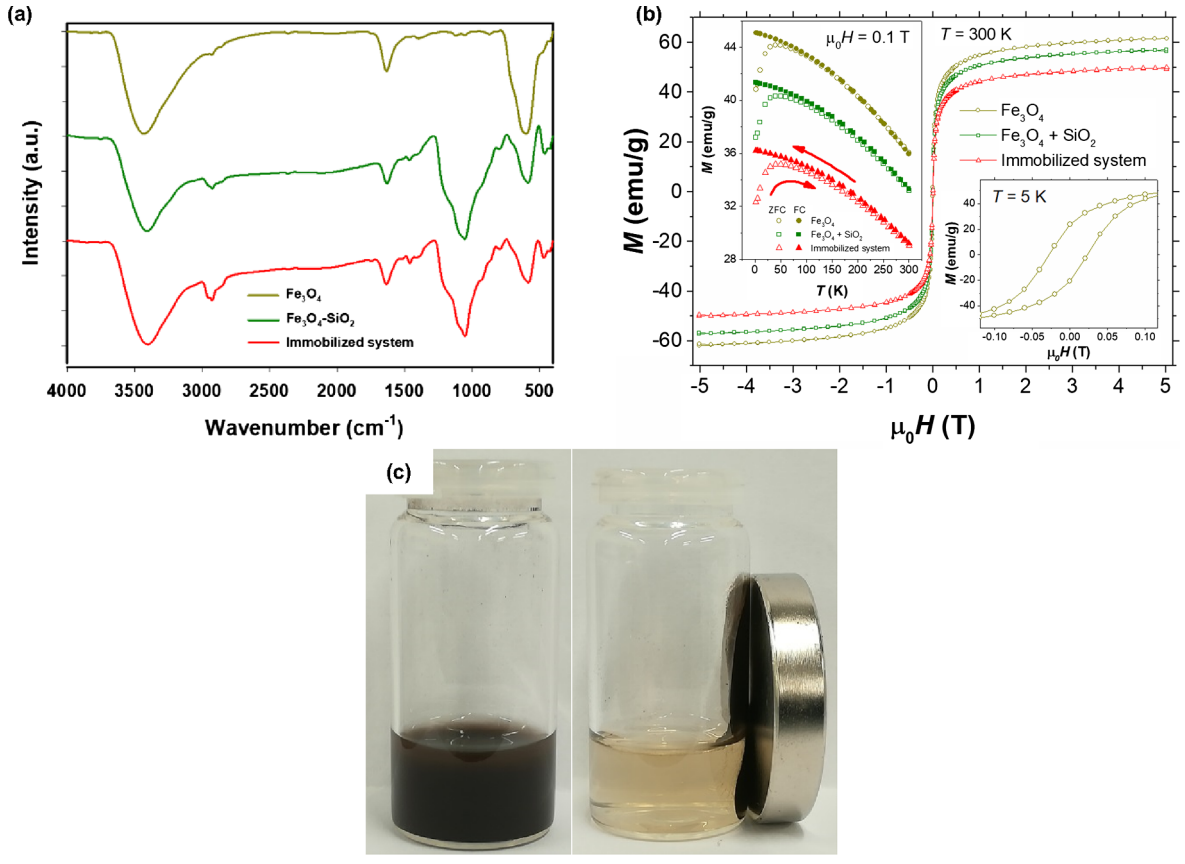

Fig. 2. (a) FTIR spectra of the magnetite, magnetite-silica core-shell material and obtained immobilized system; (b) magnetization curves of the magnetite, magnetite-silica core-shell material and immobilized system collected at room temperature. Upper inset: magnetization vs. temperature for studied materials. Lower inset: magnetization curves at 5 K for pure magnetite and (c) magnetic separation of the immobilized enzymes from the reaction mixture using an external magnetic field.

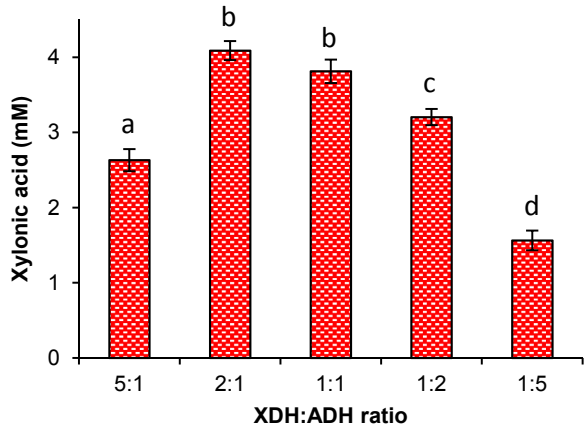

Fig. 3. Optimization of the ratio of XDH to ADH for the production of xylonic acid using co-immobilized enzymes. The letters a, b, c, d, represent significant differences among tested XDH:ADH ratios (ANOVA, $p < 0.05$).

magnetically blocked state. The ZFC curve shows a maximum at $T_{max} = 45$ K. The blocking temperature, T_B, determined from the temperature derivative of the ZFC–FC difference curve ($d(M_{ZFC}\text{-}M_{FC})/dT$) is equal to ~10 K. Moreover, as shown in Fig. 2c, the obtained biocatalytic systems were easily isolated from the reaction mixture using an external magnetic field. This significantly improved operational control of the process and the purity of the products.

3.2. Enzymes co-immobilization and effect of various XDH:ADH ratios on the production of xylonic acid

As xylose dehydrogenase and alcohol dehydrogenase have different activity and kinetics, to achieve high conversion efficiency of the substrates and simultaneously effective cofactor regeneration, as well as to minimize the required quantity of enzymes, limit side reactions and enhance the rate-limiting step, it is essential to determine the most suitable XDH:ADH ratio. The effect of variation in the XDH:ADH ratio on the productivity of xylonic acid is shown in Fig. 3. Although a higher immobilization yield (92%) was noticed for the XDH:ADH ratio 1:1, the maximum XA concentration was obtained when the xylose dehydrogenase to alcohol dehydrogenase ratio was 2:1 (immobilization yield 83%). Although the XDH:ADH ratios 2:1 and 1:1 did not differ significantly, the XDH:ADH ratio 2:1 was selected as the optimal as it gives a higher XA concentration. Deviations from this value caused lower xylose conversion due to the insufficient quantity of XDH in the system (XDH:ADH ratio 1:1–1:5) or insufficient NAD+ production/regeneration leading to an inadequate supply of NAD+ for the immobilized xylose dehydrogenase (XDH:ADH ratio 5:1). Similar observations were reported by Zhuang et al., who found that a 2:1 ratio of co-immobilized glucose dehydrogenase and NADH oxidase was the most suitable for the production of 1,3-dihydroxyacetone and cofactor regeneration [40]. An increased amount of XDH enhances the conversion both of xylose into xylonic acid and of NAD+ into NADH, even at lower NAD+ concentration, ensuring a continuous supply of NADH for the alcohol dehydrogenase and enabling efficient cofactor regeneration. Therefore, a xylose dehydrogenase to alcohol dehydrogenase ratio of 2:1 was selected as optimal for the production of XA, and was used in all further experiments.

3.3. Modelling of the effect of pH and temperature on the production of xylonic acid by co-immobilized enzymes

Eqs. (1) and (2) were used to model the dependence of xylonic acid concentration and enzyme relative activity on pH and temperature. Multivariate regression analysis based on the least squares method provided values of polynomial coefficients which produced the statistical best fit to the experimental values. The results of the calculations are given in Table 1. Figure 4 shows the actual shape of the function adjusted to the experimental values of xylonic acid concentrations.

Table 1
Model coefficients for xylonic acid concentration and activity.

i	1	2	3	4	5	6
c_i	-1.75	5.43	1.98	$-2.65 \cdot 10^{-3}$	-3.90	$-3.46 \cdot 10^{-3}$
a_i	$-4.02 \cdot 10^{2}$	$1.25 \cdot 10^{2}$	4.56	$-6.10 \cdot 10^{-2}$	-8.96	$-7.96 \cdot 10^{-2}$

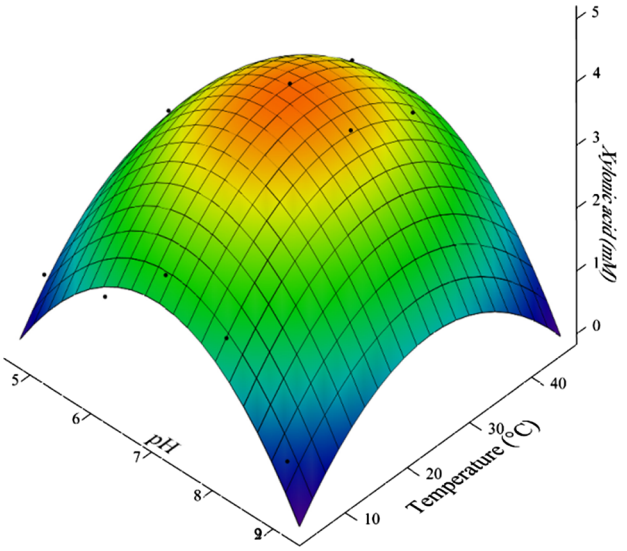

Fig. 4. Polynomial surface fit to the experimental data, according to Eqs. (1) and (2).

The statistical quality of fit is measured by the coefficient of determination R^2, which is equal to 0.864 for both functions, while the mean squared error of prediction (MSE) is 0.163 and 86.068 for concentrations and activities respectively. The value of R^2 indicates that the model selected is a good choice for describing the experimental data, while retaining a simple mathematical form. The MSE values are specific to the data measured and describe the general metric for the goodness of actual fits. The results enable the identification of optimal conditions for xylonic acid formation. The optimum is identified by finding first-order partial derivatives of the functions (1) and (2) and solving for extrema conditions by comparing them to zero value. Applying the mathematical optimum condition to (1) gives:

$$pH_{opt} = \frac{2c_6c_2 - c_3c_4}{c_4^2 - 4c_5c_6} \tag{4}$$

and

$$T_{opt} = \frac{c_4c_2 + 2c_5c_3}{c_4^2 + 4c_5c_6} \tag{5}$$

Substituting the data from Table 1 into the Eqs. (4) and (5), one obtains the optimal pH and temperature conditions for the process. The optimum values are $pH_{opt} = 6.87$ and $T_{opt} = 25.98$ °C. It should be noted that identical mathematical formulations for optimal pH and temperature can be obtained from Eq. (2). In this case the a_i coefficients could be used to find the optimal conditions, which are exactly the same as for Eq. (1) as used here.

3.4. Effect of temperature and pH on the production of xylonic acid by free and co-immobilized enzymes

It is known that the application of temperature and pH different from the enzymes' optimal values results in a decrease in their activity.

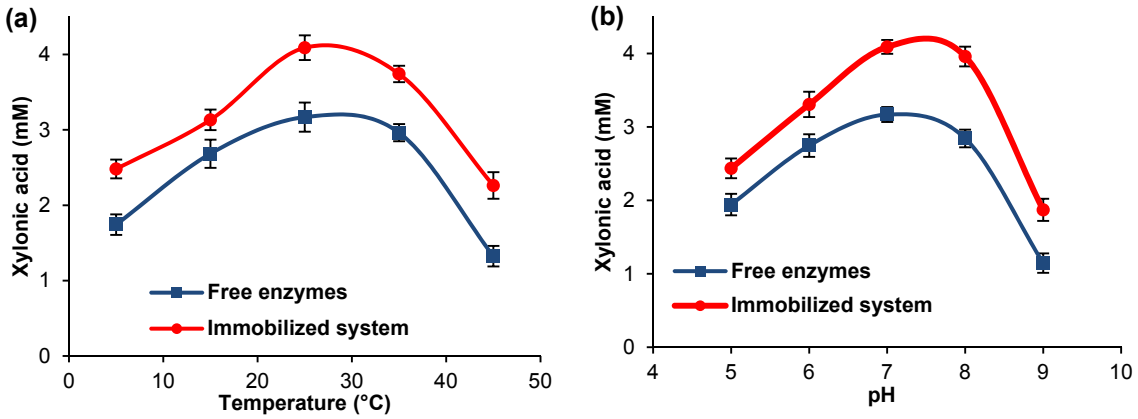

Fig. 5. Effect of (a) temperature and (b) pH on the conversion of xylose into xylonic acid catalyzed by free and co-immobilized XDH and ADH. All data are presented as means ± standard deviation.

Thus, evaluation of the pH and temperature profiles of free and co-immobilized XDH and ADH is crucial for finding the most suitable conditions for practical applications of the co-immobilized enzymes for xylose conversion and cofactor regeneration. In our previous study, xylose dehydrogenase immobilized using silica-based materials exhibited maximum activity at pH 8 and temperature 45 °C [41]. On the other hand, the highest activity of alcohol dehydrogenase immobilized on epoxy-functionalized magnetic Fe_3O_4-SiO_2 nanoparticles was found to occur at pH 7 and 30 °C [42]. Thus, a compromise must be found between these two enzymes to determine the optimal conditions for the highest xylose conversion and cofactor regeneration. Figure 5 shows the effect of pH and temperature on the productivity of xylonic acid catalyzed by free and co-immobilized enzymes. The production of xylonic acid increases as temperature and pH increase, until it reaches a maximum at pH 7 and 25 °C. Further increases in pH and temperature result in a decrease in xylose conversion. Moreover, although the free and co-immobilized enzymes display similar pH and temperature profiles, the immobilized system attains obtaining of significantly higher concentration of xylonic acid over the whole of the analyzed range. This phenomenon may be related to the changes in the enzyme microenvironment that occurred after immobilization, as reported by Secundo [43], which facilitate the activity and stability of the immobilized biocatalysts. Another possible explanation is that biomolecules are attached mainly to the hydroxyl groups of silica, which provide multipoint binding of the enzyme to the solid support and stabilize the entire biocatalyst structure. These prevent the denaturation of the biomolecules and make the system more stable over a longer time [44]. Furthermore, limited thermal and chemical denaturation of the co-immobilized enzymes, compared to the native system, restricts deactivation of the co-immobilized XDH and ADH and results in higher conversion of xylose, as presented also in Section 3.6. Similar observations have been reported by Gustafsson et al. (2015) [45] and Li et al. (2013) [46], who co-immobilized, respectively, glucose oxidase with horseradish peroxidase using a silica-based support, and glucose oxidase with xylose dehydrogenase using nafion multi-walled carbon nanotubes, observing the protective effect of the support material on the conformation of both enzymes. Furthermore, the present results indicate that the activity and stability of alcohol dehydrogenase are the limiting factors, as XDH exhibits high activity at higher pH and temperature, as mentioned above. This is in agreement with a previous study by Dreifke et al. (2017) [47], who showed that ADH is very sensitive to changes in the reaction conditions. Therefore, based on the data obtained, the optimal conditions for simultaneous xylonic acid production and *in situ* cofactor regeneration were determined to be pH 7 and temperature 25 °C.

3.5. Stability of free and co-immobilized XDH and ADH

An important advantage of immobilization is that it usually improves the enzyme's thermal and storage stability. XDH and ADH co-immobilized on magnetite-silica support exhibited significantly higher stability than the free enzymes (Fig. 6). After 30 min of incubation the co-immobilized system retained around 80% of its initial activity in conversion to xylonic acid, and after 120 min still retained 60%. Meanwhile the activity of the free enzymes dropped rapidly, to 50% after 30 min and to around 20% after 120 min (Fig. 6a). Also the inactivation constant (k_D) and half-life ($t_{1/2}$) of the co-immobilized XDH and ADH were calculated based on the linear regression slope for ln (RA) vs. time (Fig. 6b). The half-life of the immobilized system was found to be 150.7 min and was over 300% higher than for the free enzymes (49.1 min), while k_D for the tested biocatalytic system (0.0046 1/min) was 70% smaller than for the free biocatalysts (0.0141 1/min). We also evaluated the storage stability of the free and immobilized enzymes (Fig. 6c). After 20 days of storage the co-immobilized biocatalysts retained over 60% of their initial activity. That corresponds to the inactivation constant (k_D) and half-life ($t_{1/2}$) of the co-immobilized XDH and ADH of 0.027 1/day and 25.7 days, respectively (Fig. 6d). Whereas the free enzymes showed less than 20% of initial activity after 20 days (inactivation constant (k_D) and half-life ($t_{1/2}$) of 0.098 1/day and 7.1 days, respectively). The data clearly show that co-immobilization significantly improved the thermal and storage stability of the alcohol and xylose dehydrogenase. This is probably due to the binding of the biomolecules to the support, and in consequence stabilization and rigidification of the enzyme structures [48]. This protects the active sites of the biocatalysts and makes the biomolecules more resistant to reaction conditions, thus making denaturation more difficult [49]. Similar observations were made by Zhang et al. (2018) [50], who co-immobilized (*S*)-carbonyl reductase and glucose dehydrogenase using mesoporous ZnO/carbon nanoparticles. Their immobilized system retained almost 80% of its initial activity after 25 days of storage. In another study, glucose dehydrogenase was co-immobilized with ketoreductase on poly(vinyl alcohol) gel particles. After 30 days of storage the biocatalytic system retained around 80% of its catalytic properties [51]. However, in that study the enzymes were frozen and stored at –80 °C, while in our study samples were stored at a temperature of 4 °C.

3.6. Conversion of xylose to xylonic acid catalyzed by co-immobilized XDH and ADH

The bioconversion of xylose to xylonic acid was carried out using free xylose dehydrogenase as well as free and co-immobilized XDH and

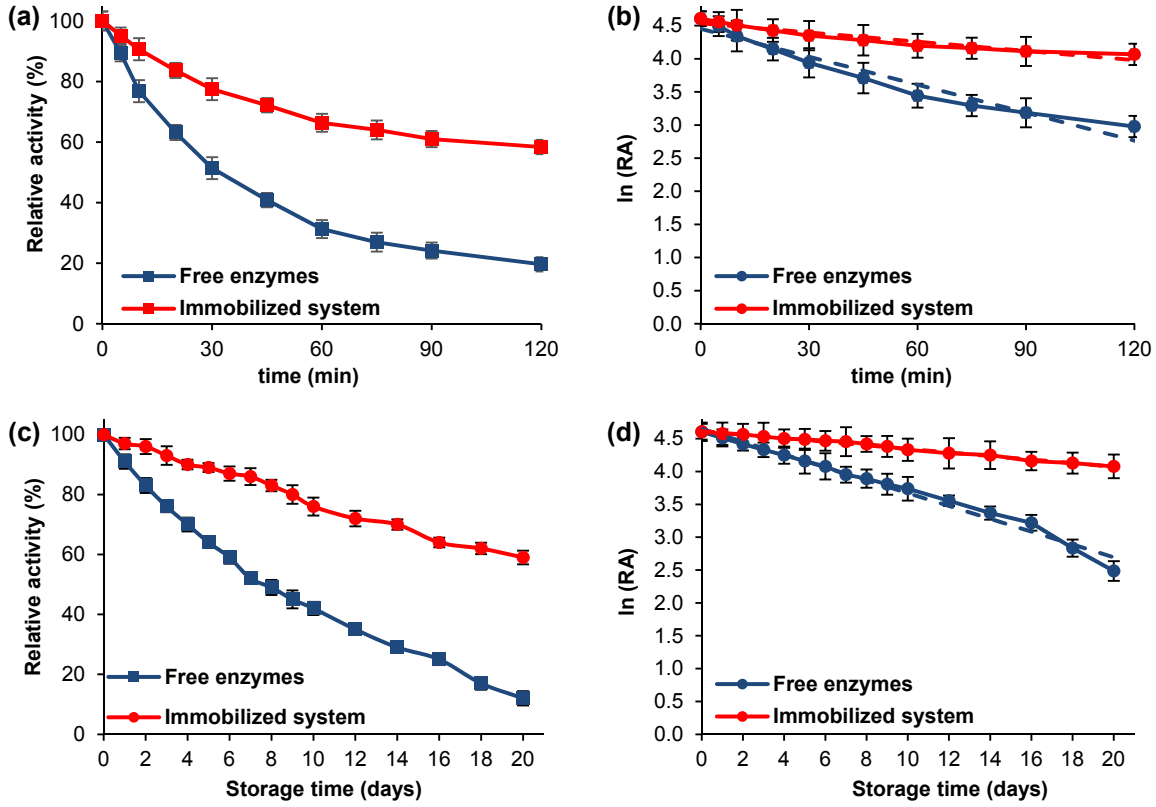

Fig. 6. (a, b) Thermal stability and (c, d) storage stability of free and co-immobilized XDH and ADH. Thermal and storage stability of free and co-immobilized enzymes were examined at optimal temperature (25 °C) and pH (7). Inactivation constants (k_D) and enzyme half-life ($t_{1/2}$) were evaluated based on the linear regression slope. All data are presented as means ± standard deviation.

ADH for *in situ* cofactor regeneration. The time courses of these reactions are presented in Fig. 7. It can be seen that reaction catalyzed by free xylose dehydrogenase produced less than 1 mM of xylonic acid after 120 min of the process that corresponds to the xylose conversion of 18.7%. By contrast, concentration of xylonic acid produced by a bi-enzymatic system of free XDH and ADH was three times higher, reaching almost 3 mM (xylose conversion of 61.9%) after 120 min of reaction that is directly related to the *in situ* cofactor regeneration, as reported earlier by Riebel et al. (2003) [52]. Furthermore, it should be emphasized that an even higher concentration of xylonic acid (4.1 mM) was obtained when the co-immobilized enzymes were used that correlates to 81.7% of xylose conversion. This may be explained by the higher stability of XDH and ADH after immobilization, as well as efficient cofactor regeneration, which caused NAD+ to be readily available for the xylose dehydrogenase. Moreover, presented results are in agreement with the data on the enzymes' stability and half-life. However, in the case of both free and co-immobilized enzymatic systems, xylose conversion increased as reaction time increased and reached its maximum after 60 min. After this time further increase in xylonic acid concentration is not observed that might be attributed mainly to the deactivation of the free enzymes and consumption of the entire substrate [53]. As data on cofactor regeneration for the production of xylonic acid by xylose dehydrogenase are limited, we are able to compare the present results only with studies dealing with cofactor regeneration systems for biomass conversion. As previously reported by Zheng and Zhang (2011) [54], Ning et al. (2014) [55], Morthensen et al. (2017) [56] and Su et al. (2018) [57], the use of cofactor regeneration based on immobilized enzymes for the production of NAD+ results in higher substrate conversion, as compared to the use of free biocatalysts. Moreover, it has been shown that a higher reaction yield can be achieved in a shorter time. Therefore, these results corroborate our observations and prove that a highly active and stable system for cofactor regeneration, based on co-immobilized enzymes, is essential to achieve high efficiencies of the conversion of selected biomass components.

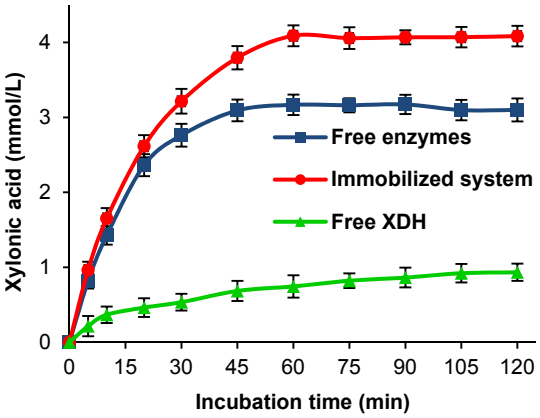

Fig. 7. Time course for the conversion of xylose to xylonic acid catalyzed by free XDH, free mixed XDH and ADH, and co-immobilized XDH and ADH. Reaction conditions: pH 7, temperature 25 °C, 5 mM of D-xylose, 5 mM of formaldehyde, 1 mM of NAD+ and 1 mM of NADH, 30 U of free or co-immobilized ADH and XDH in the ratio 2:1. All data are presented as means ± standard deviation.

3.7. Reusability and biocatalytic productivity of co-immobilized XDH and ADH

One of the main objectives of enzyme immobilization is to enhance the bioproductivity of enzymes by maximizing their recyclability over numerous catalytic cycles and continuous processes. In the present

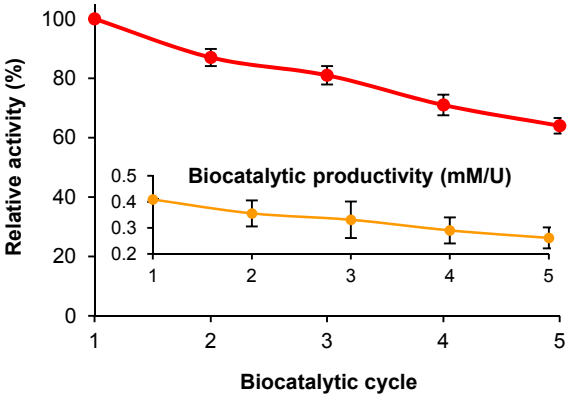

Fig. 8. Reusability of co-immobilized XDH and ADH over consecutive reaction cycles. Inset: biocatalytic productivity of xylonic acid by the immobilized system over consecutive reaction cycles. All data are presented as means ± standard deviation.

study, co-immobilized XDH and ADH were used in five consecutive reaction cycles. Over repeated reactions the catalytic activity declined steadily, reaching 65% of its initial value after five reaction cycles (Fig. 8). This corresponds to the results of enzymatic biocatalytic productivity, which also decreased over repeated runs. Nonetheless, after five cycles the biocatalytic productivity reached 1.65 mM of xylonic acid per 1 U of co-immobilized XDH used for the reaction. High activity retention was achieved due to stable binding of the enzyme to the support. This not only stabilizes the enzyme structure, but also avoids enzyme leaching: less than 5% of the enzymes was eluted from the support after each cycle. Moreover, attention should be drawn to the protective effect of the support material on the biomolecules [58]. On the other hand, the decrease in catalytic activity may be explained by inhibition of the enzyme by the reaction products, and inactivation of the biocatalysts caused by structural modification and mechanical damage [59] as well as long-term contact with formaldehyde [60]. The retention of over 65% of initial activity by co-immobilized enzymes, as reported here, is even higher than the figure previously published by Sun et al. (2009) [61], who co-immobilized formate, formaldehyde and alcohol dehydrogenase using titania nanoparticles. In that study, after five reaction cycles the co-immobilized system retained less than 50% of its initial properties, mainly due to destruction of the enzyme molecules by multiple operations under continuous stirring. In addition to the significant improvement in the enzymes' reusability, it should also be noted that reuse of the co-immobilized XDH and ADH is facilitated by the magnetic nature of the support material. By fast and simple separation from the reaction mixture and avoidance of complicated separation procedures, enzymatic activity may be preserved, as reported earlier by Zhu et al. (2014) [62].

4. Conclusions

In conclusion, in this study we have provided, for the first time, a proof-of-concept for the co-immobilization of xylose dehydrogenase and alcohol dehydrogenase using magnetite-silica core-shell particles, and its application for simultaneous xylose conversion and *in situ* cofactor regeneration. The magnetic properties of the studied materials indicate superparamagnetic behavior (with a blocking temperature of ~10 K) and reflect a small particle size and narrow particle size distribution, in good agreement with the TEM results. The effect of various operational factors on the bioproductivity of xylonic acid has been evaluated. Using co-immobilized enzymes, under optimal process conditions (pH 7, temperature 25 °C, XDH:ADH ratio 2:1, 60 min process duration) the concentration of XA obtained was over 25% higher than in the case of free enzymes. The high activity and robustness of the co-immobilized enzymes under mild reaction conditions is of particular interest, as this reduces the process costs and facilitates enzyme stability and reusability. Although immobilization did not affect the optimum pH and temperature of the bi-enzymatic system, co-immobilized XDH and ADH enable higher production of xylonic acid over broad ranges of temperature (15–35 °C) and pH (6–8). Moreover, the half-life of the co-immobilized enzymes was four times higher, and the inactivation constant four times lower, as compared to free enzymes. Furthermore, the co-immobilized enzymes also exhibited improved reusability: after five consecutive reaction cycles over 65% of their initial activity was retained, leading to a final biocatalytic productivity of 1.65 mM of xylonic acid per 1 U of xylose dehydrogenase used in the reaction. Thus, the reported data clearly show that co-immobilization of xylose dehydrogenase and alcohol dehydrogenase may be a promising strategy for long-term conversion of xylose through *in situ* cofactor regeneration. We strongly believe that these results may stimulate further developments in the obtaining of efficient, dehydrogenase-based cofactor regeneration systems for the bioconversion of valuable chemicals from renewable resources.

Acknowledgements

This work was financed and prepared as part of research project supported by the National Science Center Poland, No. 2017/27/B/ST8/01506.

References

[1] S. Lin, S. Sun, K. Wang, K. Shen, B. Ma, Y. Ren, X. Fan, Bioinspired design of alkohol dehydrogenase@nano TiO_2 microreactors for sustainable cycling of NAD+/NADH coenzyme, Nanomaterials. 8 (2018) 1–9, https://doi.org/10.3390/nano8020127.
[2] D. Weiser, F. Nagy, G. Banoczi, M. Olah, A. Farkas, A. Szilagyi, K. Laszlo, A. Gellert, G. Marosi, S. Kemeny, L. Poppe, Immobilization engineering – how to design advanced sol-gel systems for biocatalysis? Green Chem. 19 (2017) 3927–3937, https://doi.org/10.1039/c7gc00896a.
[3] P. Halling, M. Gupta, Measurement and reporting of data in applied biocatalysis, Perspect. Sci. 1 (2014) 98–109, https://doi.org/10.1016/j.pisc.2014.02.008.
[4] J. Choi, S. Han, H. Kim, Industrial applications of enzyme biocatalysis: Current status and future aspects, Biotechnol. Adv. 33 (2015) 1443–1454, https://doi.org/10.1016/j.biotechadv.2015.02.014.
[5] M. Ferrer, Biocatalysis and biotransformations, Catalysts 8 (2018) 1–6, https://doi.org/10.3390/catal8050216.
[6] T. Jesionowski, J. Zdarta, B. Krajewska, Enzyme immobilization by adsorption: A review, Adsorption 20 (2014) 801–821, https://doi.org/10.1007/s10450-014-9623-y.
[7] J. Zdarta, A.S. Meyer, T. Jesionowski, M. Pinelo, A general overview of support materials for enzyme immobilization: Characteristics, properties, practical utility, Catalysts 8 (2018) 1–27, https://doi.org/10.3390/catal8020092.
[8] J. Zdarta, L. Klapiszewski, A. Jedrzak, M. Nowicki, D. Moszynski, T. Jesionowski, Lipase B from *Candida antarctica* immobilized on a silica-lignin matrix as a stable and reusable biocatalytic system, Catalysts 7 (2017) 1–21, https://doi.org/10.3390/catal7010014.
[9] L. Pera, M. Baigori, A. Pandey, G. Castro, Biocatalysis, in: A. Pandey, R. Hofer, M. Taherzadeh, K. Nampoothiri, Ch. Larroche (Eds.), Industrial Biorefineries and White Biotechnology, Elsevier, Oxford, 2015, pp. 391–408.
[10] H. Li, W. Xiao, P. Xie, L. Zheng, Co-immobilization of enoate reductase with a cofactor-recycling partner enzyme, Enzyme Microb. Technol. 109 (2018) 66–73, https://doi.org/10.1016/j.enzmictec.2017.09.013.
[11] K. Tadyszak, A. Kertmen, E. Coy, R. Andruszkiewicz, S. Milewski, I. Kardava, B. Scheibe, S. Jurga, K. Chybczyńska, Spectroscopic and magnetic studies of highly dispersible superparamagnetic silica coated magnetite nanoparticles, J. Magn. Magn. Mater. 433 (2017) 254–261, https://doi.org/10.1016/j.jmmm.2017.03.025.
[12] X. Ji, Z. Su, G. Ma, S. Zhang, Sandwiching multiple dehydrogenases and shared cofactor between double polyelectrolytes for enhanced communication of cofactor and enzymes, Biochem. Eng. J. 137 (2018) 40–49, https://doi.org/10.1016/j.bej.2018.05.017.
[13] M. Zheng, S. Zhang, G. Ma, P. Wang, Effect of molecular mobility on coupled enzymatic reactions involving cofactor regeneration using nanoparticle-attached enzymes, J. Biotechnol. 154 (2011) 274–280, https://doi.org/10.1016/j.jbiotec.2011.04.013.
[14] H. Zhao, W. van der Donk, Regeneration of cofactors for use in biocatalysis, Curr. Opin. Biotechnol. 14 (2003) 583–589, https://doi.org/10.1016/j.copbio.2003.09.007.
[15] G. Rehn, A. Pedersen, J. Woodley, Application of NAD(P)H oxidase for cofactor regeneration in dehydrogenase catalyzed oxidations, J. Mol. Cat. B: Enzym. 134 (2016) 331–339, https://doi.org/10.1016/j.molcatb.2016.09.016.
[16] Y. Wang, L. Li, C. Ma, C. Gao, F. Tao, P. Xu, Engineering of cofactor regeneration enhances (2S,3S)-2,3-butanediol production from diacetyl, Sci. Rep. 3 (2013) 1–6, https://doi.org/10.1038/srep02643.
[17] J. Mukherjee, M. Gupta, Biocatalysis for biomass valorization, Sustain. Chem. Processes. 3 (2015) 1–5, https://doi.org/10.1186/s40508-015-0037-2.

[18] M. Jawaid, T. Paridah, N. Saba, Introduction to biomass and its composites, in: M. Jawaid, T. Paridah, N. Saba (Eds.), Lignocellulosic Fibre and Biomass-based Composite Materials, Woodhead Publishing, Sawston, 2017, pp. 1–11.

[19] T.L. de Albuquerque, I. da Silva Jr., G. de Macedo, M. Valderez Ponte Rocha, Biotechnological production of xylitol from lignocellulosic wastes: A review, Process Biochem. 49 (2014) 1779–1789, https://doi.org/10.1016/j.procbio.2014.07.010.

[20] X. Zhou, Y. Xu, Y. Shiyuan, Simultaneous bioconversion of xylose and glycerol to xylonic acid and 1,3-dihydroxyacetone from the mixture of pre-hydrolysates and ethanol-fermented waste liquid by Gluconobacter oxydans, App. Biochem. Biotechnol. 178 (2016) 1–8, https://doi.org/10.1007/s12010-015-1853-2.

[21] V. Kumar, P. Binod, R. Sindhu, E. Gnansounou, V. Ahluwalia, Bioconversion of pentose sugars to value added chemicals and fuels: Recent trends, challenges and possibilities, Bioresour. Technol. 269 (2018) 443–451, https://doi.org/10.1016/j.biortech.2018.08.042.

[22] J. Zhu, Y. Rong, J. Yang, X. Zhou, Y. Xu, L. Zhang, J. Chen, Q. Yong, S. Yu, Integrated production of xylonic acid and bioethanol from acid-catalyzed steam-exploded corn stover, Appl. Biochem. Biotechnol. 176 (2015) 1370–1381, https://doi.org/10.1007/s12010-015-1651-x.

[23] B.W. Chun, B. Dair, P.J. Macuch, D. Wiebe, C. Porteneuve, A. Jeknavorian, The development of cement and concrete additive, Appl. Biochem. Biotechnol. 129–132 (2006) 645–658, https://doi.org/10.1007/BF02685947.

[24] X. Wang, N. Xu, S. Hu, J. Yang, Q. Gao, S. Xu, K. Chen, P. Ouyang, D-1,2,4-butanetriol production from renewable biomass with optimization of synthetic pathway in engineered *Escherichia coli*, Bioresour. Technol. 250 (2018) 406–412, https://doi.org/10.1016/j.biortech.2017.11.062.

[25] X. Zhou, Y. Xu, S. Yu, Simultaneous bioconversion of xylose and glycerol to xylonic acid and 1,3-dihydroxyacetone from the mixture of pre-hydrolysates and ethanol-fermented waste liquid by *Gluconobacter oxydans*, Appl. Biochem. Biotechnol. 178 (2016) 1–8, https://doi.org/10.1007/s12010-015-1853-2.

[26] N. Tenhaef, C. Brusseler, A. Radek, R. Hilmes, P. Unrean, J. Marienhagen, S. Noack, Production of D-xylonic acid using a non-recombinant *Corynebacterium glutamicum* strain, Bioresour. Technol. 268 (2018) 332–339, https://doi.org/10.1016/j.biortech.2018.07.127.

[27] H. Liu, K.N.G. Valdehuesa, G.M. Nisola, K.R.M. Ramos, W.J. Chung, High yield production of D-xylonic acid from D-xylose using engineered *Escherichia coli*, Bioresour. Technol. 115 (2012) 244–248, https://doi.org/10.1016/j.biortech.2011.08.065.

[28] P. Richard, M. Wiebe, M. Toivari, D. Mojzita, L. Ruohonen, M. Penttila, Manufacture of xylonic acid, United States Patent, US 2012/0005788 A1, 2012.

[29] R. Cao, Y. Xu, Efficient preparation of xylonic acid from xylonate fermentation broth by bipolar membrane electrodialysis, Appl. Biochem. Biotechnol. 187 (2019) 396–406, https://doi.org/10.1007/s12010-018-2827-y.

[30] W. Hou, M. Zhang, J. Bao, Cascade hydrolysis and fermentation of corn stover for production of high titer gluconic and xylonic acids, Bioresour. Technol. 264 (2018) 395–399, https://doi.org/10.1016/j.biortech.2018.06.025.

[31] H. Zhang, G. Liu, J. Zhang, J. Bao, Fermentative production of high titer gluconic and xylonic acids from corn stover feedstock by *Gluconobacter oxydans* and techno-economic analysis, Bioresour. Technol. 219 (2016) 123–131, https://doi.org/10.1016/j.biortech.2016.07.068.

[32] F. Marpani, Z. Sarossy, M. Pinelo, A. Meyer, Kinetics based reaction optimization of enzyme catalyzed reduction of formaldehyde to methanol with synchronous co-factor regeneration, Biotechnol. Bioeng. 114 (2017) 2762–2770, https://doi.org/10.1002/bit.26405.

[33] Ł. Klapiszewski, J. Zdarta, K. Antecka, K. Synoradzki, K. Siwińska-Stefańska, D. Moszyński, T. Jesionowski, Magnetite nanoparticles conjugated with lignin: A physicochemical and magnetic study, Appl. Surf. Sci. 422 (2017) 94–103, https://doi.org/10.1016/j.apsusc.2017.05.255.

[34] M.M. Bradford, A rapid and sensitive method for the quantitation of microgram quantities of protein utilizing the principle of protein-dye binding, Anal. Biochem. 72 (1976) 248–254, https://doi.org/10.1016/0003-2697(76)90527-3.

[35] A.S.S. Ibrahim, A.A. Al-Salamah, A. Mohamed El-Toni, M.A. El-Tayeb, Y.B. Elbadawi, Cyclodextrin glucanotransferase immobilization onto functionalized magnetic double mesoporous core–shell silica nanospheres, Electronic J. Biotechnol. 17 (2014) 55–64, https://doi.org/10.1016/j.ejbt.2014.01.001.

[36] E. Ranjbakhsh, A.K. Bordbar, M. Abbasi, A.R. Khosropoura, E. Shams, Enhancement of stability and catalytic activity of immobilized lipase on silica-coated modified magnetite nanoparticles, Chem. Eng. J. 179 (2012) 272–276, https://doi.org/10.1016/j.cej.2011.10.097.

[37] J. Lee, Y. Lee, J.K. Youn, H.B. Na, T. Yu, H. Kim, S.M. Lee, Y.M. Koo, J.H. Kwak, H.G. Park, H.N. Chang, M. Hwang, J.G. Park, J. Kim, T. Hyeon, Simple synthesis of functionalized superparamagnetic magnetite/silica core/shell nanoparticles and their application as magnetically separable high-performance biocatalysts, Nano Small Micro 4 (2008) 143–152, https://doi.org/10.1002/smll.200700456.

[38] S. Datta, L.R. Christena, Y.R.S. Rajaram, Enzyme immobilization: An overview on techniques and support materials, 3 Biotech. 3 (2013) 1–9, https://doi.org/10.1007/s13205-012-0071-7.

[39] J. Zdarta, K. Antecka, A. Jędrzak, K. Synoradzki, M. Łuczak, T. Jesionowski, Biopolymers conjugated with magnetite as support materials for trypsin immobilization and protein digestion, Colloids Surf. B: Biointerfaces 169 (2018) 118–125, https://doi.org/10.1016/j.colsurfb.2018.05.018.

[40] M.Y. Zhuang, X.P. Jiang, X.M. Ling, M.Q. Xu, Y.H. Zhu, Y.W. Zhang, Immobilization of glycerol dehydrogenase and NADH oxidase for enzymatic synthesis of1,3-dihydroxyacetone with in situ cofactor regeneration, J. Chem. Technol. Biotechnol. 93 (2018) 2351–2358, https://doi.org/10.1002/jctb.5579.

[41] J. Zdarta, M. Pinelo, T. Jesionowski, A.S. Meyer, Upgrading of biomass monosaccharides by immobilized glucose dehydrogenase and xylose dehydrogenase, ChemCatChem. 10 (2018) 5164–5173, https://doi.org/10.1002/cctc.201801335.

[42] X.P. Jiang, T.T. Lu, C.H. Liu, X.M. Ling, M.Y. Zhuang, J.X. Zhang, Y.W. Zhang, Immobilization of dehydrogenase onto epoxy-functionalized nanoparticles for synthesis of (R)-mandelic acid, Int. J. Biol. Macromol. 88 (2016) 9–17, https://doi.org/10.1016/j.ijbiomac.2016.03.031.

[43] F. Secundo, Conformational changes of enzymes upon immobilisation, Chem. Soc. Rev. 42 (2013) 6250–6261, https://doi.org/10.1039/c3cs35495d.

[44] C. Mateo, J.M. Palomo, G. Fernandez-Lorente, J.M. Guisan, R. Fernandez-Lafuente, Improvement of enzyme activity, stability and selectivity via immobilization techniques, Enzym. Microb. Technol. 40 (2007) 1451–1463, https://doi.org/10.1016/j.enzmictec.2007.01.018.

[45] H. Gustafsson, A. Küchler, K. Holmberg, P. Walde, Co-immobilization of enzymes with the help of a dendronized polymer and mesoporous silica nanoparticles, J. Mater. Chem. B 3 (2015) 6174–6184, https://doi.org/10.1039/C5TB00543D.

[46] L. Li, B. Liang, F. Li, J. Shi, M. Mascini, Q. Lanf, A. Liu, Co-immobilization of glucose oxidase and xylose dehydrogenase displayed whole cell on multi walled carbon nanotube nanocomposite films modified electrode for simultaneous voltammetric detection of D-glucose and D-xylose, Biosensors Bioelectronics 42 (2013) 156–162, https://doi.org/10.1016/j.bios.2012.10.062.

[47] M. Dreifke, F.J. Brieler, M. Fröba, Immobilization of alcohol dehydrogenase from *E. coli* onto mesoporous silica for application as a cofactor recycling system, ChemCatChem. 9 (2017) 1197–1210, https://doi.org/10.1002/cctc.201700468.

[48] Y. Zhang, F. Gao, S.P. Zhang, Z.G. Su, G.H. Ma, P. Wang, Simultaneous production of 1,3-dihydroxyacetone and xylitol from glycerol and xylose using a nanoparticle-supported multi-enzyme system with *in situ* cofactor regeneration, Bioresour. Technol. 102 (2011) 1837–1843, https://doi.org/10.1016/j.biortech.2010.09.069.

[49] A. Veesar, I.B. Solangi, S. Memon, Immobilization of α-amylase onto a calix[4] arene derivative: Evaluation of its enzymatic activity, Bioorg. Chem. 60 (2015) 58–63, https://doi.org/10.1016/j.bioorg.2015.04.007.

[50] R. Zhang, J. Jiang, J. Zhou, Y. Xu, R. Xiao, X. Xia, Z. Rao, Biofunctionalized "kiwifruit-assembly" of oxidoreductases in mesoporous ZnO/carbon nanoparticles for efficient asymmetric catalysis, Adv. Mater. 30 (2018), https://doi.org/10.1002/adma.201705443 article number 1705443.

[51] T. Petrovicova, K. Markosova, Z. Hegyi, I. Smonou, M. Rosenberg, M. Rebros, Co-immobilization of ketoreductase and glucose dehydrogenase, Catalysts 8 (2018) 168–177, https://doi.org/10.3390/catal8040168.

[52] B.R. Riebel, P.R. Gibbs, W.B. Wellborn, A.S. Bommarius, Cofactor regeneration of both NAD+ from NADH and NADP+ from NADPH:NADH oxidase from *Lactobacillus sanfranciscensis*, Adv. Synth. Catal. 345 (2003) 707–712, https://doi.org/10.1002/adsc.200303039.

[53] L. Wang, H. Zhang, C.B. Ching, Y. Chen, R. Jiang, Nanotube-supported bioproduction of 4-hydroxy-2-butanone via *in situ* cofactor regeneration, Appl. Microbiol. Biotechnol. 94 (2012) 1233–1241, https://doi.org/10.1007/s00253-011-3699-z.

[54] M. Zheng, S. Zhang, Immobilization of glycerol dehydrogenase on magnetic silica nanoparticles for conversion of glycerol to value-added 1,3-dihydroxyacetone, Biocatal. Biotransform. 29 (2011) 278–287, https://doi.org/10.3109/10242422.2011.631212.

[55] C. Ning, E. Su, Y. Tian, D. Wei, Combined cross-linked enzyme aggregates (combi-CLEAs) for efficient integration of a ketoreductase and a cofactor regeneration system, J. Biotechnol. 184 (2014) 7–10, https://doi.org/10.1016/j.jbiotec.2014.05.004.

[56] S.T. Morthensen, S.B. Sigurdardóttir, A.S. Meyer, H. Jørgensen, M. Pinelo, Separation of xylose and glucose using an integrated membrane system for enzymatic cofactor regeneration and downstream purification, J. Memb. Sci. 523 (2017) 327–335, https://doi.org/10.1016/j.memsci.2016.10.017.

[57] E. Su, M. Yang, C. Ning, X. Ma, S. Deng, Magnetic combined cross-linked enzyme aggregates (Combi-CLEAs) for cofactor regeneration in the synthesis of chiral alcohol, J. Biotechnol. 271 (2018) 1–7, https://doi.org/10.1016/j.jbiotec.2018.02.007.

[58] M. Vinoba, M. Bhagiyalakshmi, S.K. Jeong, Y.I. Yoon, S.C. Nam, Immobilization of carbonic anhydrase on spherical SBA-15 for hydration and sequestration of CO_2, Coll. Surf. B Biointerface 90 (2012) 91–96, https://doi.org/10.1016/j.colsurfb.2011.10.001.

[59] J. Zdarta, K. Antecka, R. Frankowski, A. Zgoła-Grześkowiak, H. Ehrlich, T. Jesionowski, The effect of operational parameters on the biodegradation of bisphenols by *Trametes versicolor* laccase immobilized on *Hippospongia communis* spongin scaffolds, Sci. Total. Environ. 615 (2018) 784–795, https://doi.org/10.1016/j.scitotenv.2017.09.213.

[60] Y. Pocker, H. Li, Kinetics and mechanism of methanol and formaldehyde interconversion and formaldehyde oxidation catalyzed by liver alcohol dehydrogenase, Adv. Exp. Med. Biol. 284 (1991) 315–325, https://doi.org/10.1007/978-1-4684-5901-2_34.

[61] Q. Sun, Y. Jiang, L. Zhang, X. Sun, J. Li, Green and efficient conversion of CO_2 to methanol by biomimetic coimmobilization of three dehydrogenases in protamine-templated titania, Ind. Eng. Chem. Res. 48 (2009) 4210–4215, https://doi.org/10.1021/ie801931j.

[62] Y.T. Zhu, X.Y. Ren, Y.M. Liu, Y. Wei, L.S. Qing, X. Liao, Covalent immobilization of porcine pancreatic lipase on carboxyl-activated magnetic nanoparticles: Characterization and application for enzymatic inhibition assays, Mat. Sci. Eng. C 38 (2014) 278–285, https://doi.org/10.1016/j.msec.2014.02.011.